Biometals (2021) 34:1007–1016
https://doi.org/10.1007/s10534-021-00323-y

Anti-*Pseudomonas aeruginosa* biofilm activity of tellurium nanorods biosynthesized by cell lysate of *Haloferax alexandrinus* GUSF-1(KF796625)

Jyothi Judith Alvares · Irene Jeronimo Furtado

Received: 9 January 2021 / Accepted: 7 June 2021 / Published online: 26 June 2021

Abstract *Pseudomonas aeruginosa*, an opportunistic human pathogen, is a major health concern as it grows as a biofilm and evades the host's immune defenses. Formation of biofilms on catheter and endotracheal tubes demands the development of biofilm-preventive (anti-biofilm) approaches and evaluation of nanomaterials as alternatives to antibiotics. The present study reports the successful biosynthesis of tellurium nanorods using cell lysate of *Haloferax alexandrinus* GUSF-1 (KF796625). The black particulate matter had absorption bands at 0.5 and 3.6 keV suggestive of elemental tellurium; showed x-ray diffraction peaks at 2θ values 24.50°, 28.74°, 38.99°, 43.13°, 50.23° and displayed a crystallite size of 36.99 nm. The black nanorods of tellurium were an average size of 40 nm × 7 nm, as observed in transmission electron microscopy. To our knowledge, the use of cell lysate of *Haloferax alexandrinus* GUSF-1 (KF796625) as a green route for the biosynthesis of tellurium nanorods with a *Pseudomonas aeruginosa* biofilm inhibiting capacity is novel to haloarchaea. At 50 μg mL^{-1}, these tellurium nanorods exhibited 75.03% in-vitro reduction of biofilms of *Pseudomonas aeruginosa* ATCC 9027, comparable to that of ciprofloxacin, which is used in treatment of *Pseudomonas* infections. Further, the observed ability of these nanoparticles to inhibit the formation of *Pseudomonas* biofilms is worthy of future research perusal.

Keywords *Haloferax alexandrinus* GUSF-1 (KF796625) · Tellurium nanorods · *Pseudomonas aeruginosa* · Anti-biofilm

Introduction

The planktonic Gram-negative *Pseudomonas aeruginosa* (*P. aeruginosa*) grows in a matrix that enables its cells to adhere together as robust biofilms and cause major health problems of concern in immunocompromised patients. (Johnson 2008). Additionally, the microbe loves to bind to urinary catheters and endotracheal tubes. The biofilm growth enables *P. aeruginosa* to evade host immune defenses, antibiotic treatment and promote chronic diseases (Wagner and Iglewski 2008). This biofilm of the microbe on catheter and endotracheal tubes demands the development of new biofilm-preventive (anti-biofilm)

Authors dedicate the paper to Prof. Suneela Mavinkurve, former Head, Microbiologyand Dean, Faculty of Life Sciences and Environment, Goa University-India.

Supplementary Information The online version contains supplementary material available at https://doi.org/10.1007/s10534-021-00323-y.

J. J. Alvares · I. J. Furtado (✉)
Department of Microbiology, Goa University, Taleigao Plateau, Goa 403206, India
e-mail: ijfurtado@unigoa.ac.in

approaches, among which evaluation of nanomaterials as alternatives to antibiotics is gaining importance (Lemire et al. 2013). Silver nanoparticles is explored for their antibacterial activity against human and mammalian pathogens such as *P. aeruginosa* ATCC 9027, *Bordetella bronchiseptica* ATCC 4617, *B. subtilis* ATCC 6633, *S. aureus* ATCC 6538P, *S. epidermidis* ATCC 12228, *E. coli* ATCC 8739, *S. typhimurium* ATCC 14028 (Patil et al. 2014). Tellurium nanoparticles (TeNPs) are also tested for their antibiotic potential against *Escherichia coli* (Lin et al. 2012). Efficacy of tellurium nanoparticles in inhibiting Gram-negative and Gram-positive bacteria is reported by Srivastava et al. 2015, who concluded that their effect towards Gram-negative organisms was found to be higher. On the other hand, studies dealing with inhibition of anti-biofilms of *P. aeruginosa* using tellurium nanoparticles are few (Gómez-Gómez et al. 2019).

The production of TeNPs through bio-reduction of tellurite to elemental tellurium using: whole cells, cell free culture supernatants and enzymes of various prokaryotic eubacteria are recorded by Baesman et al. (2007) and in Archaea, like *Halococcus salifodinae* BK3 (Srivastava et al. 2015). Tellurium nanoparticles with shapes of wires, pencils and cubes have been characterized through TEM imaging (Lin et al. 2012). Such biosynthetically produced nanoparticles are desired because they are expected not to require addition of toxic chemical stabilizers to avoid aggregation of particulate matter (Honary et al. 2011), this benefit is argued to give the biological processes an advantage in green technology over chemical processes and hence, superior (Barabadi et al. 2018).

Various mechanisms are recorded for the biosynthetic formation of elemental tellurium such as: resistant cultures accept the metalloid oxyanions as electrons in the respiratory chain (Borghese et al. 2004); enzymes such as nitrate reductases reduce and produce elemental tellurium which is precipitated as black deposits in various cellular compartments (Taylor 1999) and the NADH-dependent tellurite reductase conversion of tellurite by *Halococcus salifodinae* BK3, a member of Haloarchaea (Srivastava et al. 2015). Recent research observations on toxicity of TeNPs towards pathogens, although not fully understood, is credited to its oxidation in the media, which results in the formation of oxyanion tellurite with strong oxidizing property, resulting in the formation of deleterious reactive oxygen species which are toxic to most microorganisms, particularly Gram-negative bacteria (Tremaroli et al. 2007; Lloyd-Jones et al. 1994).

Haloferax alexandrinus GUSF-1 (KF796625) a haloarchaeon from a salt pan of Goa-India is reported to produce biotechnologically relevant molecules (Alvares and Furtado 2021) and exhibits inherent high resistance to hydrocarbon pollutants (Raghavan and Furtado 2005). The culture is also reported to perform inorganic metal conversions of Mn (II) to rhodochrosite, (Naik and Furtado 2019) and biosynthesize silver nanomaterial with antibacterial properties against human and mammalian pathogens (Patil et al. 2014). With this in mind, we investigated the ability of the cell lysate of *Haloferax alexandrinus* GUSF-1 (KF796625) to biosynthesize tellurium nanomaterial and successfully demonstrated their ability to inhibit formation of biofilms by *P. aeruginosa,* growing in polystyrene micro-titer plates and catheter tubing.

Materials and methods

Chemicals and reagents

All chemicals and reagents used were of analytical grade, obtained from Himedia Laboratories, India. Aqueous 1 mM potassium tellurite (K_2TeO_3) was prepared by dissolving the salt in ultra-pure water (Millipore, Direct Q-3).

Cell lysate of *Haloferax alexandrinus* GUSF-1

The culture was maintained at room temperature (RT, 28–32 °C) on agar slopes of 25% NaCl Tryptone Yeast Extract (NTYE) containing (g/ L): $MgSO_4 \cdot 7H_2O$, 20; KCl, 5; $CaCl_2 \cdot 2H_2O$ 0.2; Yeast Extract, 3; Tryptone, 5; NaCl, 250 and pH 7, adjusted by 1 N NaOH (Raghavan and Furtado 2004). Cell mass (100 mg of wet weight) of *Haloferax alexandrinus* GUSF-1 (GenBank accession number KF796625) was harvested by centrifuging the culture grown in NTYE broth at 42 °C at 10,000 rpm, 4 °C for 10 min, using an Eppendorf centrifuge 5804 R, Germany. The cell pellet obtained was washed thrice in sterile 15% (w/v) NaCl, subjected to osmotic lysis and freed of cell debris by centrifuging.

Biosynthesis of TeNPs by cell lysate of *Haloferax alexandrinus* GUSF-1

Equal quantities of cell lysate and 1 mM K_2TeO_3 were mixed and kept standing at RT and visually monitored for any color change. The particulate material thus formed was collected at 10,000 rpm, 4 °C for 40 min, using an Eppendorf centrifuge 5804 R, Germany. The pellet obtained was washed with sterile water, dried at 80 °C, pulverized and stored in a vial at RT. The culture was also grown in NTYE in the presence and absence of 1 mM K_2TeO_3 and a lead acetate paper strip (Fisher Scientific, Pittsburgh, PA) was placed in the headspace of the flask to qualitatively determine if any hydrogen sulfide was produced.

Fourier Transform Infrared Spectrometer (FT-IR) analysis

The FT-IR spectrum of the sample was obtained with a Fourier Transform Infrared Spectrometer (FT- IR) (IRPrestige-21 Shimadzu) by individually mixing the dried cell lysate/sample with KBr powder in a 1:10 ratio (w/w). The KBr pellet was analyzed in the range of 4000–400 cm^{-1} at a resolution of 4 cm^{-1}.

Characterization of the nanoparticles

Scanning Electron Microscopy (SEM) and Energy-dispersive X-ray Spectroscopy (EDX)

The fine powder of the prepared sample was deposited on carbon stubs as a very thin layer, coated with gold and mounted on a sample holder approximately 50 mm from the bottom of the sputter head. JEOL JSM-5800LV scanning and EDX spectroscope, Japan was used for analysis.

X-ray diffraction analysis

A thin film of the sample was prepared by placing about 1 g of the individual sample on a separate indented slide and pressed with a clean slide. The slide was placed in the Rigaku Miniflex X-ray diffractometer and scanned from 30 to 80 °C operated at a voltage of 40 kV, current 20 mA with Cu Ka radiation of 1.541 °A. The data was plotted using Origin 8 software and Full Width at Half Maximum value was obtained. The crystallite size of the nanoparticles was calculated using Scherrer's equation $D = K\lambda/\beta\text{Cos}\ \theta$ where D is the grain size, K is a constant taken to be 0.94, λ is the wavelength of the x-ray radiation, β is the full width at half maximum and θ is the angle of diffraction.

Transmission electron microscopy and selected area electron diffraction

The finely ground sample was suspended in ethanol and 10 µL of the colloidal solution was drop-coated on carbon-coated copper TEM grids and air-dried. The morphology images were obtained using Philips (Model-CM200) Transmission Electron Microscope at a resolution of 2.4 °A and operated at an accelerating voltage of 200 keV. Selected area electron diffraction (SAED) analysis was also carried out using the TEM microscope. The size of the particles in the images was measured using the Image J software and the mean value reported.

Activity of tellurium nanoparticles against biofilms of *P. aeruginosa* ATCC 9027

A 1:100 dilution of 18 h old culture of *P. aeruginosa* ATCC 9027 pre-grown in Luria Bertani (LB) broth at 37 °C (O'Toole 2011) was transferred into fresh LB medium, with 0.2% glucose to induce growth as biofilm (Srey et al. 2013). An aliquot of 50 µL was dispensed out in each well of a 96 well micro-titer plate and different volumes of TeNPs were added to 5 different wells to give a final concentration of 10, 20, 30, 40, 50 µg mL^{-1} (v/v). The final volume was then made to 100 µL using LB containing 0.2% glucose and the plate was incubated at 37 °C for 18 h. A well with 50 µg mL^{-1} of ciprofloxacin and another well having medium along with the culture was also maintained. After 18 h of growth, free cells and the spent medium was discarded, wells were rinsed with sterile distilled water to take off loosely attached cells and residual medium. The plate was then left to dry overnight. To quantify the biofilms, an aliquot of 125 µL of 0.1% aqueous solution of crystal violet was added to stain the biofilms and discarded after 15 min. This was followed by the addition of 125 µL of 30% (v/v) acetic acid. The plate was further incubated at RT for 15 min and the solubilized crystal violet was measured at 550 nm against 30% (v/v) acetic acid as the reference. Control of *P. aeruginosa* ATCC 9027 was maintained. Similarly, biofilm formation on a sterile

catheter tubing made of a polyurethane material was also studied. Two 1 cm pieces were cut under aseptic conditions and exposed to *P. aeruginosa* ATCC 9027 in the absence and presence of 50 μg mL^{-1} (v/v) of TeNPs and growth of biofilms was also evaluated.

The percent (%) inhibition was calculated as

$$\frac{A_{550}\,(\text{biofilm growth}) - A_{550}\,(\text{Biofilm growth in presence of TeNPs/Ciprofloxacin})}{A_{550}\,(\text{biofilm growth})} \times 100$$

All the experiments were carried out in triplicates. Using IBM-SPSS 23 software, USA, a one-way analysis of variance (ANOVA) was performed to assess the variation.

Results and discussion

Microbial culturing

The haloarchaeon, *Haloferax alexandrinus* GUSF-1, used in this study, is an inhabitant of solar salt from a salt pan located at Goa-India (Sequeira 1992). The culture grows optimally at 42 °C, thrives in 35% NaCl and at saturation. The cells are also seen to produce an orange pigment (Supplementary Fig. 1). During the course of growth, the culture is reported to produce several biomolecules with characteristics of carotenoid type of molecules (Alvares and Furtado 2018).

Biosynthesis of TeNPs

In the present case, the cells of the culture accumulated black particulate matter when grown in the presence of 1 mM K_2TeO_3 from day 3 onwards which increased in intensity when visually monitored up to six days of growth (Fig. 1). Normal growing cultures produced hydrogen sulfide as evidenced from the blackening of the lead acetate paper (Fig. 2). Interestingly, the lead acetate paper did not blacken in the flask where the culture was growing in the presence of 1 mM K_2TeO_3, thus indicating that the process of reduction of tellurite to elemental tellurium (involved the use of hydrogen sulfide that was produced by the growing cultures. Involvement of hydrogen sulfide and the sulfate/sulfur assimilation pathway is reported as an important cellular route mediating tellurite toxicity and intracellular accumulation of tellurium in *Saccharomyces cerevisiae* (Ottosson et al. 2010). Other reports implicating the role of enzyme tellurite reductase in the bio reduction process are also available among eubacteria and haloarchaea (Calderón et al. 2006; Srivastava et al. 2015).

In order to avoid the additional step to release the accumulated nanomaterial from cells, we ventured to carry out the reduction process using the easily obtained cell lysate by osmotic shocking of whole cells of *Haloferax alexandrinus* GUSF-1. Incubation of the cell lysate of *Haloferax alexandrinus* GUSF-1 with an equal quantity of aqueous solution of 1 mM K_2TeO_3, at RT, also led to the formation of black precipitate within 48 h, which accumulated and settled at the bottom of the tube, a preliminary indication that tellurite was reduced to its elemental form (Fig. 3). Formation and accumulation of black precipitates, like in our case, is indicative of reduced elemental

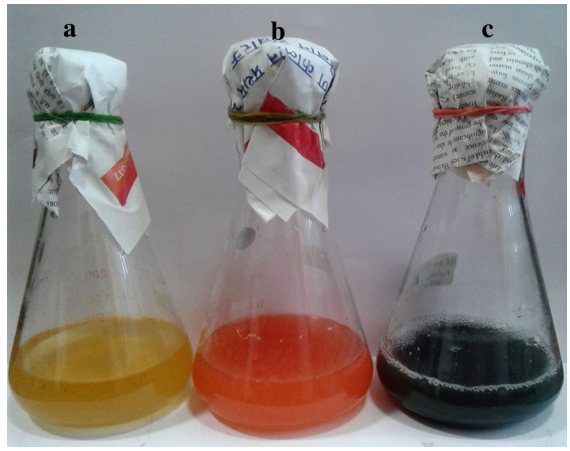

Fig. 1 **a** NTYE with 1 mM K_2TeO_3; **b** *Haloferax alexandrinus* GUSF-1 growing in NTYE; **c** *Haloferax alexandrinus* GUSF-1 growing in NTYE with 1 mM K_2TeO_3

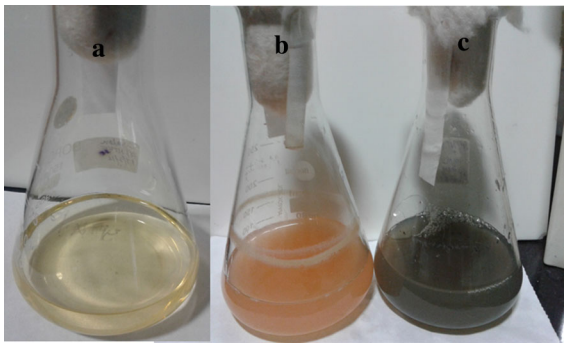

Fig. 2 Lead acetate paper test **a** NTYE with 1 mM K_2TeO_3 (no blackening of lead acetate paper); **b** *Haloferax alexandrinus* GUSF-1 growing in NTYE (blackening of lead acetate paper) **c** *Haloferax alexandrinus* GUSF-1 growing in NTYE with 1 mM K_2TeO_3 (no blackening of lead acetate paper)

tellurium and has been reported in a number of eubacteria. Yurkov et al. (1996) reported that the growth of obligately aerobic photosynthetic bacteria, *Erythrobacter litoralis* in medium supplemented with K_2TeO_3 resulted in formation of a black color indicating that tellurite reduction was caused by bacterial activities and not by the direct chemical reaction with the compounds in the medium. Similarly, bacteria such as *Escherichia coli* are reported to grow in the presence of K_2TeO_3 and produce black deposits that do not diffuse in the medium (Summers and Jacoby 1977). A single report on tellurite reduction from among haloarchaea is also available attributing the black coloration in the medium to the

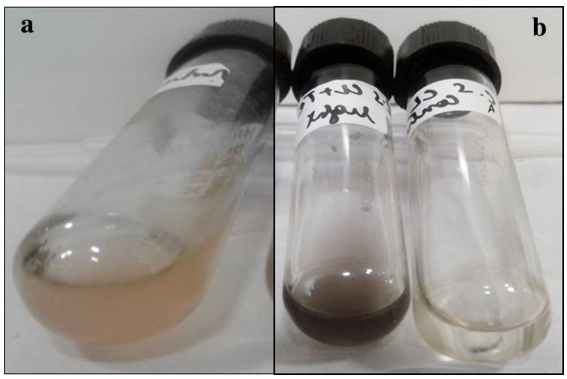

Fig. 3 **a** Cell lysate of *Haloferax alexandrinus* GUSF-1; **b** (Left) Incubation of the cell lysate with 1 mM K_2TeO_3 leads to formation of black particulate material; (Right) 1 mM K_2TeO_3

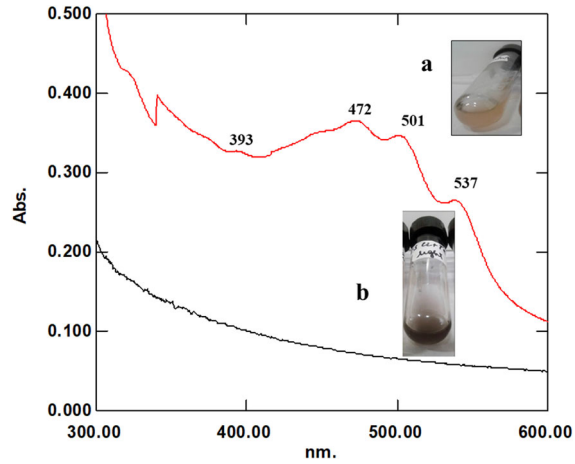

Fig. 4 Visible spectrum of cell lysate of **a** *Haloferax alexandrinus* GUSF-1; **b** *Haloferax alexandrinus* GUSF-1 incubated with 1 mM K_2TeO_3

formation of elemental tellurium (Srivastava et al. 2015).

On the other hand, the cell lysate which was obtained from whole cells was mauve and as observed in Fig. 4a, the spectrophotometric profile showed peaks corresponding to 393, 472, 501, 537, which on addition of K_2TeO_3 disappeared as elemental tellurium was progressively formed (Fig. 4b). These peaks are of bacterioruberin and its derivatives, and earlier characterized as antioxidants; active in saline and non-saline milieu (Alvares and Furtado 2018; Alvares and Furtado 2021). Hence, the mechanism of reducing tellurite to elemental tellurium by the cell lysate of *Haloferax alexandrinus* GUSF-1, is, therefore, attributed to these C_{50} carotenoids and their derivatives. The role of antioxidant phenolic compounds from the stem bark extract of *Shorea roxburghii* are reported in the reduction of silver nitrate to silver nanoparticles (Subramanian et al. 2013).

FTIR analysis

As the cell lysate of *Haloferax alexandrinus* GUSF-1 was expected to contain biomolecules, the FTIR spectrum of the cell lysate in the presence of elemental tellurium was seen to manifest shifting of absorption peaks of cell lysate located at 3400 cm^{-1}, 2966 cm^{-1},

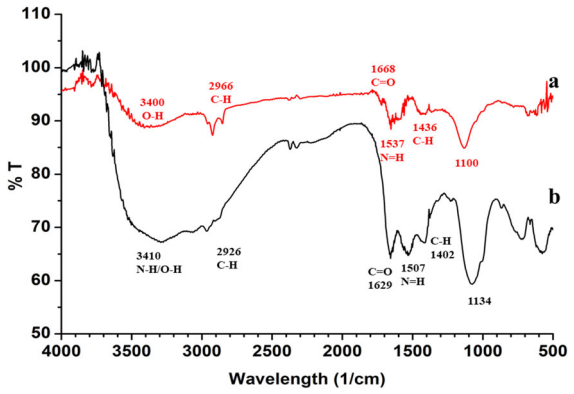

Fig. 5 FTIR spectrum of cell lysate of **a** *Haloferax alexandrinus* GUSF-1 and **b** *Haloferax alexandrinus* GUSF-1 incubated with 1 mM K_2TeO_3

1668 cm^{-1}, 1537 cm^{-1}, 1436 cm^{-1} and 1100 cm^{-1} to 3410 cm^{-1}, 2926 cm^{-1}, 1629 cm^{-1}, 1507 cm^{-1}, 1402 cm^{-1}, and 1134 cm^{-1} (Fig. 5a, b). This shift of peaks was similar to that seen in case of silver nanoparticles biosynthesized by this same culture as reported by Patil et al. (2014). The peaks at 3400/3410 were assigned to stretching vibration of bonded and non-bonded –O–H groups; the band at 2966/2926 cm^{-1} was associated with the C–H stretching; the peaks between 1668/1629 was associated to the C=O stretching of the carbonyl groups and 1537/1507 cm^{-1} to N–H group. Furthermore, the peaks between at 1436/1402 cm^{-1} corresponding to vibrations have been attributed to $–CH_2–$, $–CH_3–$, –OH, C–C, C–O, C–O–C groups. In addition, the peak at 1110/1134 cm^{-1} indicated the presence of functional groups possibly coming from sugars and polysaccharides (Nakanishi and Solomon 1977; Coates 2000; Barabadi et al. 2014). We concluded that these groups associated with elemental tellurium were from the biomolecules present in the cell lysate and also the attached bacterioruberin and its derivatives which reduced tellurite to black elemental tellurium during the biosynthesis process. Further it is postulated that they aid as capping agents and help avoid steric aggregation. While reports implicating bio-reducing of metal ions to form nanoparticles are available among eubacteria and haloarchaea (Calderón et al. 2006; Srivastava et al. 2015), none of these, however, used cell lysate, making this as the first report of the use of haloarchaeal cell lysate and more specifically cell lysate of *Haloferax alexandrinus* GUSF-1 for reduction of tellurite to elemental tellurium.

Characterization of tellurium nanoparticles

As is depicted in Fig. 6a, the diffraction peaks in XRD profiles at 2θ values 24.50°, 28.74°, 38.99°, 43.13° and 50.23° corresponded to the (100), (101), (012), (110) and (202) planes and corroborated with JCPDS card No 085-0563 indicating hexagonal structure of crystalline tellurium with the average crystallite size of 36.99 nm obtained by Scherrer's equation. The EDAX peaks at 0.5 and 3.6 keV confirmed the presence of elemental tellurium (Fig. 6b). Morphological characterization by TEM showed tellurium nanorods with an average length size of 40 nm and an average width of 7 nm (Fig. 7a, b). Adhesion of these nanorods leading to the formation of rosettes was also observed (Fig. 7c). Selected area electron diffraction (SAED) image exhibited diffraction rings corresponding to the (101), (012) and (110) directions of the hexagonal phase of tellurium can be collated to the XRD peaks of tellurium (Fig. 7d). Synthesis of tellurium nanorods, nanorice, nanopencils and irregular nanospheres are reported using either whole cells, cell-free supernatants and enzymes from Gram-positive and Gram-negative proteobacteria (Basnayake et al. 2001; Borghese et al. 2004; Klonowska et al. 2005; Baesman et al. 2007; Zare et al. 2012), but never using aqueous cell lysate. Even, the only report available on haloarchaea biosynthesizing tellurium nanoparticles uses whole cells of *Halococcus salifodinae* BK3 (Srivastava et al. 2015). Therefore, this study is the first report on biosynthesis of tellurium nanoparticles from potassium tellurite employing cell lysate of the haloarchaeon *Haloferax alexandrinus* GUSF-1. The process is simple, cost-effective, quick and the down streaming/collections of nanomaterial does not require chemical, physical or thermal inputs. The tellurium nanorods produced by *Haloferax alexandrinus* GUSF-1 with average length of 40 nm and width of 7 nm are comparable than those produced inside the cells of haloarcheaon *Halococcus salifodinae* BK3 (44 nm × 10 nm) (Srivastava et al. 2015) but smaller than those produced by *Pseudomonas pseudoalcaligenes* strain Te (185 nm × 20 nm) (Shakibaie et al. 2017). The tellurium rods giving rise to rosettes corroborates with large rosettes composed of several tellurium nanorods reported in eubacterial biogenesis by Baesman et al.

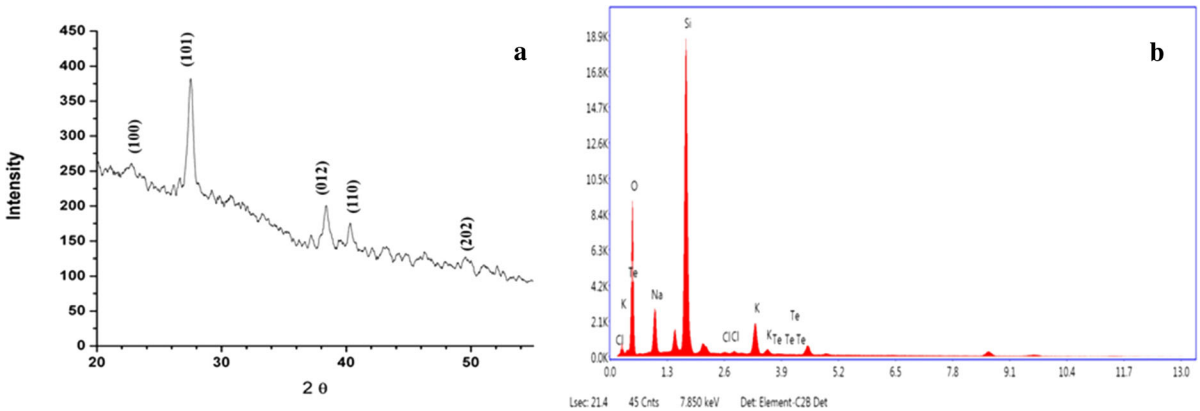

Fig. 6 **a** XRD pattern and **b** EDX profile of the biosynthesized tellurium nanoparticles

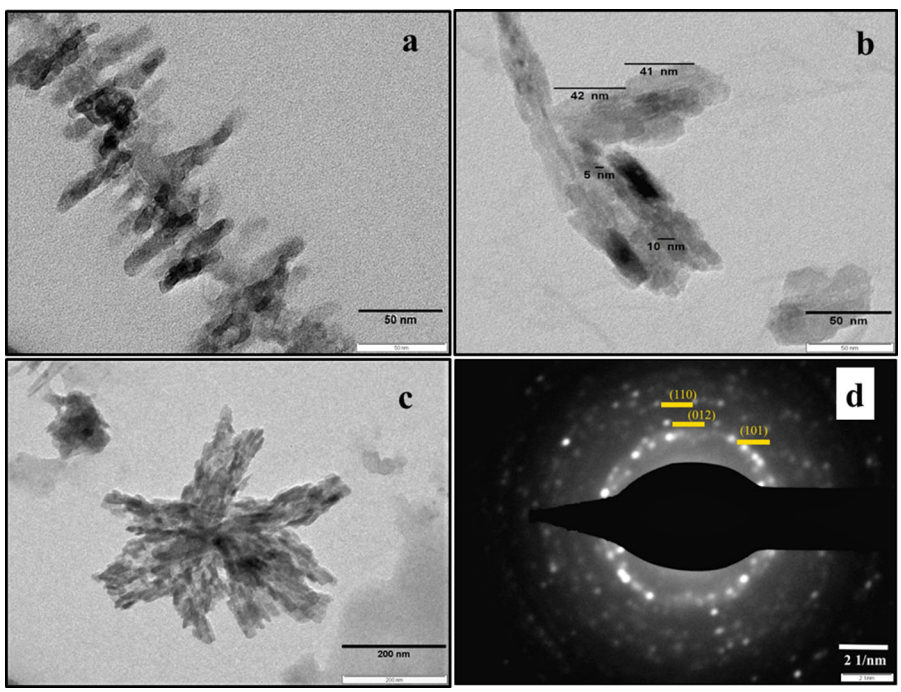

Fig. 7 **a–b** TEM micrograph showing tellurium nanorods (different views); **c** rosette pattern **d** SAED profile of tellurium nanorods

(2007) and Shakibaie et al. (2017), and attributed to the adherence due to electrostatic interaction.

The anti-biofilm potential of TeNPs

According to the Centers for Disease Control and Prevention (CDC), *P. aeruginosa* ATCC 9027 is the fourth most commonly isolated nosocomial pathogen; accounting for 10% of all hospital-acquired infection owing to its increased antibiotic resistance (Wu and Li 2015), and its ability to form biofilms (Rasamiravaka et al. 2015). Varying concentrations of tellurium nanorods (10 to 50 μg mL^{-1}) affected biofilm formation in *P. aeruginosa* ATCC 9027 monitored by the crystal violet assay (Fig. 8a). One-way ANOVA revealed a dose-dependent inhibition of the biofilms ($p < 0.001$) as compared to culture grown in absence of tellurium nanoparticles, and was almost equal with

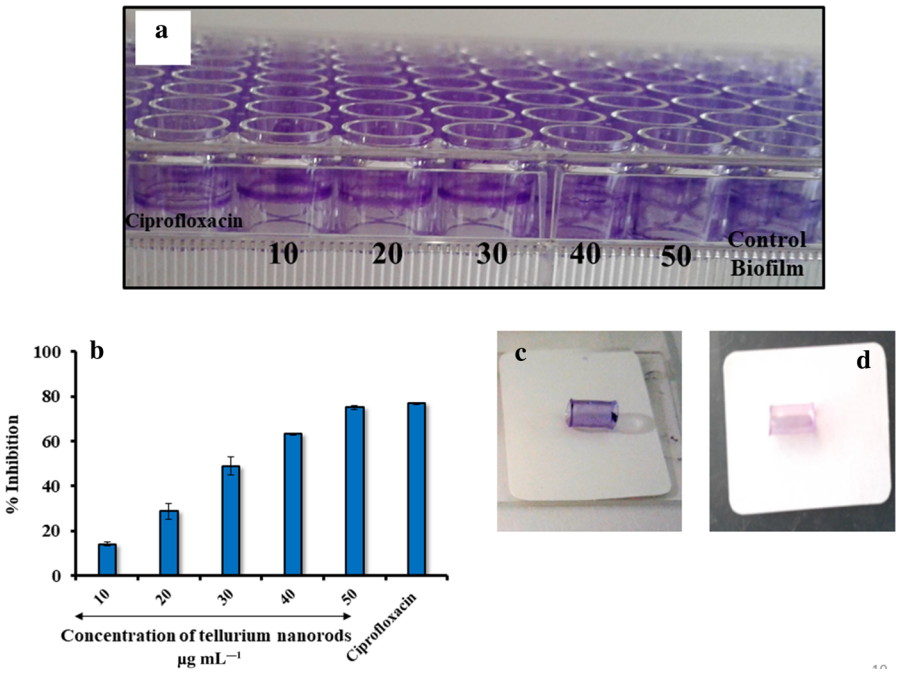

Fig. 8 **a** Anti-biofilm activity of the antibiotic ciprofloxacin(well 1) and varying concentrations of TeNPs on P. *aeruginosa* ATCC 9027 (well 2-6); extreme right is the control biofilm **b** Percent inhibition of the biofilm formation ($n = 3$; values presented as mean ± SD; $p < 0.001$); **c** biofilm attachment to the polyurethane tube in the absence of TeNPs; **d** reduction of biofilm growth in the presence of TeNPs

the inhibition displayed by equal quantity of ciprofloxacin (76.78% v/s 75.03%), first line antibiotic for treatment of *Pseudomonas* infections. (Fig. 8b). This role of the antibacterial activity of tellurium nanorods is attributed to its oxidation in the media, which results in the formation of oxyanion tellurite (TeO_3^{2-}), which in turn gives rise to toxic deleterious reactive oxygen species (Tremaroli et al. 2007) which are toxic to most microorganisms, particularly Gram-negative bacteria (Lloyd-Jones et al. 1994). Biogenically synthesized tellurium nanorods at 175 mg L^{-1} eradicated preformed biofilms of P. *aeruginosa* (Zonaro et. al 2015), while inhibition of P. *aeruginosa* ATCC 9027 in this study was achieved at a much lower concentration of tellurium nanorods and hence, expected to be effective in deterring the growth of the biofilm. This preliminary result is worthy of being explored as a catheter wash solution as also seen in Fig. 8c, d wherein the biofilm attachment and formation is reduced on the polyurethane tubes in the presence of tellurium nanorods (63.73%). Moreover, tellurium nanoparticles are observed and reported to be non-toxic as compared to sodium tellurite and silver nanoparticles to humans by Lin et al. (2012) in their study on metal ion absorption with renal cell line; LLC-PK1 cells. Most biogenic tellurium nanorods are reported to exhibit an MBC (minimum bactericidal concentration) between 125 and 500 mg L^{-1} against different clinical isolates such as *S. aureus*, *P. aeruginosa*, *S. typhimurium* and *K. pneumonia* (Zare et al. 2012), through formation of reactive oxygen species (ROS) as a part of their killing strategy (Tremaroli et al. 2007). In this study it's therefore, possible that tellurium nanoparticles induce ROS to kill the *P. aeruginosa* ATCC 9027 and stop their multiplication or/and effect their adhesion and matrix forming properties.

Conclusion

Tellurium nanorods were successfully biosynthesized using the cell lysate of the haloarchaeon *Haloferax alexandrinus* GUSF-1 (KF796625). Bacterioruberin and its derivatives from the cell lysate were seen to be involved in the biosynthesis of the nanomaterial. The tellurium nanorods organized into a rosette pattern and exerted an anti-biofilm potential against *P. aeruginosa* ATCC 9027. Further, a reduction of the biofilm production on catheter tubing material was seen. To the best of our knowledge, the use of cell lysate for the synthesis of tellurium nanorods nanomaterial in the haloarchaeal domain is novel.

Acknowledgements The authors wish to thank IIT-Bombay, for the TEM facility, National Institute of Oceanography, Goa, for the XRD profiling, University Science Instrumentation Centre (USIC), Goa University, for SEM-EDX and Department of Chemistry, Goa University, for FT-IR analysis.

Declarations

Conflict of interest The authors declare that they have no conflict of interest.

References

Alvares JJ, Furtado IJ (2018) Extremely halophilic Archaea and Eubacteria are responsible for free radical scavenging activity of solar salts of Goa—India. Global J Biosci Biotechnol 7(2):242–254

Alvares JJ, Furtado IJ (2021) Characterization of multicomponent antioxidants from *Haloferax alexandrinus* GUSF-1 (KF796625). 3 Biotech 11:58. https://doi.org/10.1007/s13205-020-02584-9

Baesman SM, Bullen TD, Dewald J, Zhang D, Curran S, Islam FS, Beveridge TJ, Oremland RS (2007) Formation of tellurium nanocrystals during anaerobic growth of bacteria that use Te oxyanions as respiratory electron acceptors. Appl Environ Microbiol 73(7):2135–2143. https://doi.org/10.1128/AEM.02558-06

Barabadi H, Honary S, Ebrahimi P, Mohammadi MA, Alizadeh A, Naghibi F (2014) Microbial mediated preparation, characterization and optimization of gold nanoparticles. Braz J Microbiol 45(4):1493–1501. https://doi.org/10.1590/s1517-83822014000400046

Barabadi H, Kobarfard F, Vahidi H (2018) Biosynthesis and characterization of biogenic tellurium nanoparticles by using *Penicillium chrysogenum* PTCC 5031: a novel approach in gold biotechnology. Iran J Pharm Res 17(Suppl2):87–97

Basnayake RST, Bius JH, Akpolat OM, Chasteen TG (2001) Production of dimethyl telluride and elemental tellurium by bacteria amended with tellurite or tellurate. Appl Organomet Chem 15(6):499–510

Borghese R, Borsetti F, Foladori P, Ziglio G, Zannoni D (2004) Effects of the metalloid oxyanion tellurite (TeO_3^{2-}) on growth characteristics of the phototrophic bacterium *Rhodobacter capsulatus*. Appl Environ Microbiol 70(11):6595–6602. https://doi.org/10.1128/AEM.70.11.6595-6602.2004

Calderón IL, Arenas FA, Pérez JM, Fuentes DE, Araya MA, Saavedra CP, Tantaleán JC, Pichuantes SE, Youderian PA, Vásquez CC (2006) Catalases are NAD(P)H-dependent tellurite reductases. PLoS ONE 1(1):e70. https://doi.org/10.1371/journal.pone.0000070

Coates J (2000) Interpretation of infrared spectra, a practical approach. In: Meyers RA (ed) Encyclopedia of analytical chemistry. Wiley, New York, pp 10815–10837

Gómez-Gómez B, Arregui L, Serrano S, Santos A, Pérez-Corona T, Madrid Y (2019) Selenium and tellurium-based nanoparticles as interfering factors in quorum sensing-regulated processes: violacein production and bacterial biofilm formation. Metallomics 11(6):1104–1114. https://doi.org/10.1039/c9mt00044e

Honary S, Ghajar K, Khazaeli P, Shalchian P (2011) Preparation, characterization and antibacterial properties of silver-chitosan nanocomposites using different molecular weight grades of chitosan. Trop J Pharm Res 10:69–74

Johnson LR (2008) Micro colony and biofilm formation as a survival strategy for bacteria. J Theor Biol 251:24–34. https://doi.org/10.1016/j.jtbi.2007.10.039

Klonowska A, Heulin T, Vermeglio A (2005) Selenite and tellurite reduction by *Shewanella oneidensis*. Appl Environ Microbiol 71:5607–5609. https://doi.org/10.1128/AEM.71.9.5607-5609.2005

Lemire JA, Harrison JJ, Turner RJ (2013) Antimicrobial activity of metals: mechanisms, molecular targets and applications. Nat Rev Microbiol 11(6):371–384. https://doi.org/10.1038/nrmicro3028

Lin ZH, Lee CH, Chang HY, Chang HT (2012) Antibacterial activities of tellurium nanomaterials. Chem Asian J 7(5):930–934. https://doi.org/10.1002/asia.201101006

Lloyd-Jones G, Osborne M, Ritchie DA, Strike P, Hobman JL, Brown NL, Rouch DA (1994) Accumulation and intracellular fate of tellurite-resistant *Escherichia coli*: a model for mechanism of resistance. FEMS Microbiol Lett 118:113–120

Naik S, Furtado I (2019) Formation of Rhodochrosite by *Haloferax alexandrinus* GUSF-1. J Clust Sci 30:1435–1441. https://doi.org/10.1007/s10876-019-01586-9

Nakanishi K, Solomon PA (1977) Infrared absorption spectroscopy, 2nd edn. Holden-Day, San Francisco

O'Toole GA (2011) Microtiter dish biofilm formation assay. J vis Exp 47:2437. https://doi.org/10.3791/2437

Ottosson LG, Logg K, Ibstedt S, Sunnerhagen P, Käll M, Blomberg A, Warringer J (2010) Sulfate assimilation mediates tellurite reduction and toxicity in *Saccharomyces cerevisiae*. Eukaryot Cell 9(10):1635–1647. https://doi.org/10.1128/EC.00078-10

Patil S, Fernandes J, Tangsali RB, Furtado I (2014) Exploitation of *Haloferax alexandrinus* for biogenic synthesis of silver nanoparticles antagonistic to human and lower mammalian pathogens. J Clust Sci 25:423–433. https://doi.org/10.1007/s10876-013-0621-0

Radzig MA, Nadtochenko VA, Koksharova OA, Kiwi J, Lipasova VA, Khmel IA (2013) Antibacterial effects of silver nanoparticels on gram-negative bacteria: influence on the growth and biofilm formation, mechanisms of action. Colloids Surf B 102:300–306. https://doi.org/10.1016/j.colsurfb.2012.07.039

Raghavan TM, Furtado I (2004) Occurrence of extremely halophilic archaea in sediments from the continental shelf of west coast of India. Curr Sci India 86:1065–1067

Raghavan TM, Furtado I (2005) Expression of carotenoid pigments of haloarchaeal cultures exposed to aniline. Environ Toxicol 20(2):165–169. https://doi.org/10.1002/tox.20091

Rasamiravaka T, Labtani Q, Duez P, El Jaziri M (2015) The formation of biofilms by *pseudomonas aeruginosa*: a review of the natural and synthetic compounds interfering

with control mechanisms. BioMed Res Int 2015:759348. https://doi.org/10.1155/2015/759348

Sequeira F (1992) Microbiological study of salt pans of Goa. Master of Science dissertation. Goa University, India

Shakibaie M, Adeli-Sardou M, Mohammadi-Khorsand T, Zeydabadi-Nejad M, Amirafzali E, Amirpour-Rostami S, Ameri A, Forootanfar H (2017) Antimicrobial and antioxidant activity of the biologically synthesized tellurium nanorods; a preliminary in vitro study. Iran J Biotechnol 15(4):268–276. https://doi.org/10.15171/ijb.1580

Srey S, Jahid IK, Ha S-D (2013) Biofilm formation in food industries: a food safety concern. Food Control 31(2):572–585. https://doi.org/10.1016/j.foodcont.2012.12.001

Subramanian R, Subbramaniyan P, Raj V (2013) Antioxidant activity of the stem bark of *Shorea roxburghii* and its silver reducing power. Springerplus 2:28. https://doi.org/10.1186/2193-1801-2-28

Srivastava P, Nikhil EVR, Braganca JM, Kowshik M (2015) Anti-bacterial TeNPs biosynthesized by haloarcheaon *Halococcus salifodinae* BK3. Extremophiles 19:875–884. https://doi.org/10.1007/s00792-015-0767-9

Summers AO, Jacoby GA (1977) Plasmid-determined resistance to tellurium compounds. J Bacteriol 129:276–281

Taylor DE (1999) Bacterial tellurite resistance. Trends Microbiol 7:111–115

Tremaroli V, Fedi S, Zannoni D (2007) Evidence for a tellurite-dependent generation of reactive oxygen species and absence of a tellurite-mediated adaptive response to oxidative stress in cells of *Pseudomonas pseudoalcaligenes* KF707. Arch Microbiol 187(2):127–135. https://doi.org/10.1007/s00203-006-0179-4

Wagner VE, Iglewski BH (2008) *P. aeruginosa* biofilms in CF infection. Clin Rev Allergy Immunol 35:124–134. https://doi.org/10.1007/s12016-008-8079-9

Wu M, Li X (2015) *Klebsiella pneumoniae* and *Pseudomonas aeruginosa*. In: Tang Y-W, Sussman M, Liu D, Poxton I, Schwartzman J (eds) Molecular medical microbiology, vol 87, 2nd edn. Academic Press, New York, pp 1547–1564

Yurkov V, Jappe J, Vermeglio A (1996) Tellurite resistance and reduction by obligately aerobic photosynthetic bacteria. Appl Environ Microbiol 62(11):4195–4198

Zare B, Faramarzi MA, Sepehrizadeh Z, Shakibaie M, Rezaie S, Shahverdi AR (2012) Biosynthesis and recovery of rod-shaped tellurium nanoparticles and their bactericidal activities. Mater Res Bull 47(11):3719–3725. https://doi.org/10.1016/J.Materresbull.2012.06.034

Zonaro E, Lampis S, Turner RJ, Qazi SJS, Vallini G (2015) Biogenic selenium and tellurium nanoparticles synthesized by environmental microbial isolates efficaciously inhibit bacterial planktonic cultures and biofilms. Front Microbiol 6(584). https://doi.org/10.3389/fmicb.2015.00584